Open Journal of Civil Engineering, 2025, 15(2), 249-270
https://www.scirp.org/journal/ojce
ISSN Online: 2164-3172
ISSN Print: 2164-3164

The Impact of Vertical Scaling on the Estimation of Fractal Dimension of Slope Failures in Opencast Mine

Dina Kon[1], Jisen Shu[2], Dave Mbako[3]

[1]School of Mines, China University of Mining and Technology, Xuzhou, China
[2]State Key Laboratory of Resources and Mine Safety, China University of Mining & Technology, Xuzhou, China
[3]School of Naval, Architecture, Ocean and Civil Engineering, Shanghai Jiao Tong University, Shanghai, China
Email: dinakon25@gmail.com

How to cite this paper: Kon, D.N., Shu, J.S. and Mbako, D. (2025) The Impact of Vertical Scaling on the Estimation of Fractal Dimension of Slope Failures in Opencast Mine. *Open Journal of Civil Engineering*, **15**, 249-270.
https://doi.org/10.4236/ojce.2025.152014

Received: February 21, 2025
Accepted: June 27, 2025
Published: June 30, 2025

Abstract

This study investigates the effect of vertical scaling on fractal dimension (FD) estimation for failure surfaces in opencast mines to improve surface roughness characterization for slope stability analysis. Fractal analysis has become an essential tool in geotechnical engineering, yet the impact of scaling on FD estimation remains underexplored. Seven fractal analysis methods were evaluated: Box Counting Method (BCM), Power Spectrum (PS), Variogram (V), Structure Function (SF), Triangular Prism Method (TPM), Differential Box Counting (DBC), and Detrended Fluctuation Analysis (DFA). These methods were applied using MATLAB to a failure surface from the Mashamba West mine, examining scaling factors from fine to coarse. The results show that vertical scaling significantly affects FD estimates. BCM and DBC exhibited decreasing FD values as scaling increased, with BCM values ranging from1 1.649 at a scaling factor of 0.1 to 1.0367 at 10. In contrast, PS, Variogram, and SF demonstrated increasing FD values, with PS rising from 1.2744 at 0.1 to 2.8701 at 10. TPM produced stable FD values (~2.025) across all scaling factors, indicating robustness to scaling. DFA showed a gradual increase in FD, from 1.666 at 0.1 to 2.6224 at 10, suggesting moderate sensitivity to scaling. These findings highlight the need for careful method selection based on the scale and complexity of the surface, as different methods exhibit varying performance at various scales. This study contributes to a better understanding of the scaling effects on FD estimation and supports a more accurate characterization of failure surfaces in geotechnical applications.

Keywords

Fractal Dimension, Vertical Scaling, Failure Surfaces, Surface Complexity, Surface Roughness, Surface Characterization

1. Introduction

Fractal and multifractal methods have become essential tools for analyzing the complexity of rough surfaces in various fields, including geosciences [1] [2], medical image analysis [3], fracture mechanics [4], tribology [5], and manufacturing [6]. These methods provide a robust framework for characterizing surface roughness by quantifying its irregularities through the fractal dimension (FD), a key parameter that measures the geometric complexity of surfaces. Fractal dimension (FD) estimation is critical for understanding the physical properties of surfaces, especially in applications like opencast mining, where surface complexity plays a crucial role in slope stability and failure mechanisms.

In surface analysis, the primary stochastic variable is typically the topographical height, while in image analysis, it is the grayscale intensity of pixels [7]. Both surfaces are often self-affine, meaning their vertical and horizontal scaling differs upon magnification. Vertical scaling refers to the change in the vertical dimension of a surface when it is magnified, and it is a key factor in the analysis [8]. Necessitating specialized techniques for accurate FD estimation. This distinction between vertical and horizontal scaling adds complexity to the analysis, significantly when vertical scaling is adjusted to enhance certain surface features or emphasize specific details. Accurate estimation of FD is crucial in applications such as opencast mining, where surface roughness impacts slope stability and failure behavior.

Several methods have been developed to estimate FD, each with its strengths, limitations, and sensitivities to scaling. The Box Counting Method (BCM) [9]-[13] is one of the most widely used techniques due to its simplicity and ease of implementation. However, it has been shown to underestimate FD for highly complex surfaces, mainly when applied to discretized surfaces. The Differential Box Counting method (DBC) [14]-[16] addresses this limitation by refining the algorithm to improve accuracy for discretized versions of continuous surfaces. BCM and DBC are popular for image analysis and surface characterization, but vertical scaling strongly influences performance.

In addition to BCM and DBC, other methods have been employed to analyze surface roughness, such as the Power Spectrum (PS) [17]-[19], Structure Function (SF) [20], and Variogram (V) [18] [21]-[23]. The PS and SF methods are effective at capturing features across multiple scales. PS utilizes Fourier transforms to analyze frequency content, while SF measures squared height differences over specific distances. These methods are widely applied to time-series data and line profiles, although they require careful adaptation for two-dimensional surface analysis. The Variogram method, which measures spatial autocorrelation, has been successfully applied to geological and geotechnical contexts, offering insights into surface roughness in these settings.

Another commonly used technique is the Triangular Prism Method (TPM) [24]-[27], which is intuitive and conceptually linked to the ruler method introduced by Mandelbrot [28]-[31]. TPM is particularly efficient in analyzing rough surfaces; however, it is sensitive to vertical scaling and image contrast adjustments, which can lead to FD underestimation. Modifications to TPM, such as those proposed by Sun *et al.* [26], have reduced some of these biases. Still, challenges remain when applying TPM to self-affine surfaces with arbitrary vertical scaling. The Detrended Fluctuation Analysis (DFA) [32] [33], an extension of Hurst's R/S method [34]-[36], is another important technique. DFA is useful for identifying long-range correlations and trends in rough surfaces and is known for its balance between sensitivity and robustness in surface roughness analysis.

While fractal and multifractal methods have proven effective for analyzing surface roughness across various fields, the influence of vertical scaling on FD estimation remains a significant and pressing challenge. Although previous studies have applied these methods to surface characterization, many fail to adequately address the variability introduced by vertical scaling, especially in geotechnical contexts such as failure zones in opencast mining. Vertical scaling alters how surface features are perceived and quantified, particularly on self-affine failure surfaces with distinct scaling behaviors along their vertical and horizontal axes. This highlights the need for further research and innovation in this area.

This study specifically examines the impact of vertical scaling on FD estimation by evaluating seven methods, such as BCM, DBC, PS, SF, V, TPM, and DFA, in the context of opencast mining. The research focuses on failure surfaces from the Mashamba West mine, which is known for its complex geological structures and history of slope failures. The paper aims to determine how different vertical scaling factors affect the accuracy and robustness of these methods in characterizing surface roughness. The potential impact of this research is significant, as it could provide valuable insights for improving slope stability analysis in mining operations, thereby enhancing safety and efficiency.

2. Mathematical Analysis of Vertical Scaling in the Triangular Prism Method

This section quantitatively assesses the TPM applied to slope failures in opencast mine. These surfaces can be modeled as fractional Brownian motion, which allows us to apply the mathematical framework developed in [35].

In this technique, the failure surface is defined on a square grid consisting of $N \times N$ squares with sides a_0 (corresponding to pixels if image analysis is concerned) $N = 2^{n_0}$, n_0 determined by the resolution of the surface measurements or images. Consider a single square in the grid with a side a. The heights of the points p_α are denoted h_α $\alpha: 1 \to 4$ and numbered counter-clockwise. These heights represent the elevation of the failure surface at each point. The vectors connecting the points are denoted v_α, $\alpha: 1 \to 4$ describing the square in a counter-clockwise direction. Their vertical component is indicated as Δh_α. The formula for the surface area in the TPM can be calculated as:

$$S_i = \frac{1}{4}\left(\|v_1 \times v_2\| + \|v_2 \times v_3\| + \|v_3 \times v_4\| + \|v_4 \times v_1\|\right) \tag{1}$$

For a fractional Brownian motion surface, which is used to model the failure surface, $\sigma_a = ca^H$ where H the Hurst exponent is, C is an unknown factor that introduces vertical scaling into the problem. The expected value of the total surface area is found to be:

$$\langle S_{Tot} \rangle = 1 + \sqrt{\frac{\pi}{2}} ca^{H-1} \mathrm{e}^{\frac{a^2 - 2H}{2c^2}} erfc\left(\frac{a^{1-H}}{\sqrt{2}c}\right) \tag{2}$$

The fractal dimension is found by taking the limit:

$$D = \lim_{a \to 0} \frac{\log S_{Tot}}{\log a} \tag{3}$$

Substituting $a = 2^{-n}$, we get: $D = 3 - H$.

This relationship between H and D is correct for surfaces defined on a 2D grid and is independent of the unknown factor c. This implies that the TPM is independent of vertical scaling for failure surfaces in its ideal mathematical formulation. However, in practice, the maximum value n is defined by the resolution of the surface measurements or images. The following function n, dependent on the parameters H c, is defined:

$$D(n; H, c) = 2 + \frac{\log_2\left(1 + \sqrt{\frac{\pi}{2}} c2^{(1-H)n} \mathrm{e}^{\frac{2n(H-1)}{2c^2}} erfc\left(\frac{2^{n(H-1)}}{\sqrt{2}c}\right)\right)}{n} \tag{4}$$

To eliminate the unknown parameter c, the total variance of the surface height over the square grid with side one is calculated:

$$\langle h^2 \rangle = c^2 v(H) \tag{5}$$

where $v(H)$ is a function H involving gamma and hypergeometric functions. This analysis provides a framework for understanding how vertical scaling affects fractal dimension estimation for failure surfaces using the TPM. While TPM is theoretically independent of vertical scaling, practical limitations in measurement resolution can introduce scaling dependencies.

The method was initially based on the assumption that these surfaces follow fractional Brownian motion (FBM). However, real-world surfaces often exhibit anisotropic roughness, geological heterogeneity, and mixed scaling behaviors, which may deviate from ideal FBM assumptions. To address these limitations, the study incorporates the following improvements:

Assessing the Combined Impact of Vertical and Horizontal Scaling

Instead of analyzing vertical scaling in isolation, this TPM method examines the interaction between vertical and horizontal scaling and their combined influence on fractal dimension (FD) estimates (Figure 1). This joint evaluation of these two dimensions provides a more comprehensive understanding of surface characteristics that FBM-based models may not fully capture. By doing so, this approach refines the scaling independence assumptions in TPM analysis, offering more profound insights into how geological features influence FD estimations, thereby enhancing the knowledge of the audience.

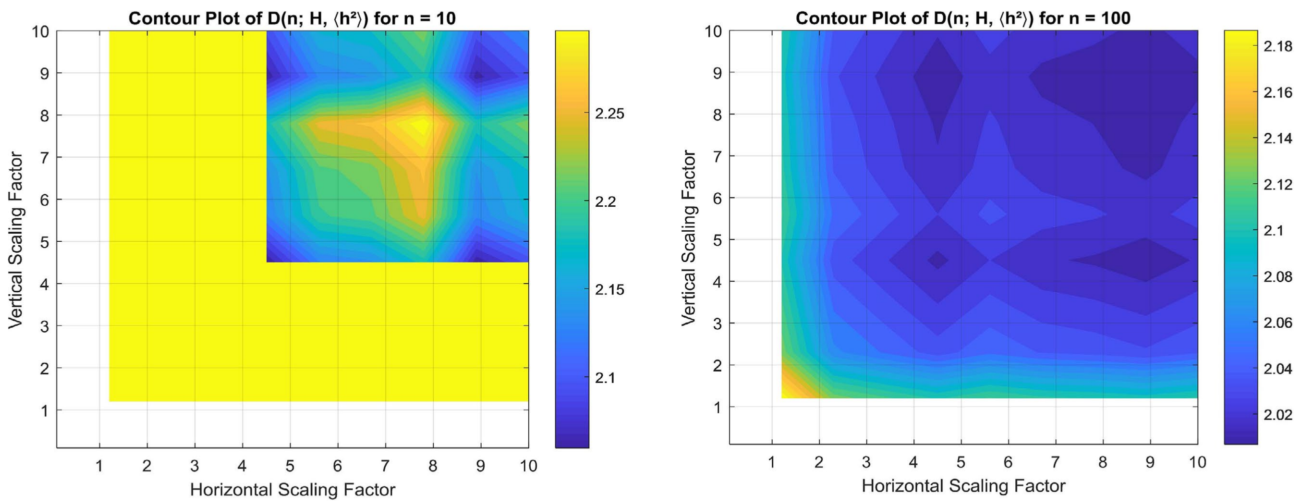

Figure 1. Interaction between vertical and horizontal scaling by TPM.

These contour plots illustrate the influence of horizontal and vertical scaling factors on the fractal dimension (D) estimated using the Triangular Prism Method (TPM). At lower vertical scaling factors, D shows significant variability, as indicated by the deviation of contour lines from an ideal vertical alignment. As the vertical scaling factor increases, the contours become more stable, suggesting reduced dependency on vertical exaggeration. This highlights the resolution dependence of TPM-derived fractal dimensions and the need for careful scaling considerations in geotechnical applications.

3. Methodology

This research investigates surface roughness and fractal geometry to slope failures at the Mashamba West mine, a site characterized by complex geological conditions and a history of instability. The study evaluates the impact of vertical scaling factors on fractal dimension (FD) estimation, a key parameter in assessing slope stability within geotechnical applications. By analyzing how vertical scaling influences fractal measurements, the research enhances the reliability of FD-based approaches, contributing to a more accurate understanding of slope stability.

High-resolution JPEG images of failure surfaces were obtained during field surveys to facilitate fractal analysis. These images underwent a series of preprocessing steps to optimize their suitability for quantitative analysis. First, they were converted into a 14-bit grayscale format to improve contrast and ensure smoother intensity transitions, which is essential for precise pixel intensity analysis. Next, a

Gaussian filter was applied to reduce noise by averaging pixel values within a defined neighborhood, effectively minimizing high-frequency noise while preserving critical image features. To enhance resolution, bicubic interpolation was used to increase the number of pixels, resulting in smoother and more detailed images, which is particularly beneficial for capturing intricate surface features. Finally, an edge detection algorithm was implemented to highlight significant surface features, improving characterization in subsequent fractal analysis.

Following preprocessing, vertical scaling factors were introduced to simulate vertical exaggeration or suppression conditions. This step addresses variability introduced by different scaling conditions, which is particularly relevant for self-affine surfaces in geotechnical applications. By systematically modifying the vertical scaling, the study evaluates its influence on fractal dimension estimations and assesses the robustness of different fractal analysis methods under varying scaling conditions.

To achieve this, the study examines the performance of seven fractal analysis methods: Box Counting Method (BCM), Differential Box Counting (DBC), Power Spectrum (PS), Variogram (V), Structure Function (SF), Triangular Prism Method (TPM), and Detrended Fluctuation Analysis (DFA). These methods are evaluated based on their sensitivity to vertical scaling and effectiveness in characterizing surface roughness within the opencast mining environment. The comparative analysis provides insights into the applicability of each method for geotechnical investigations, particularly in slope stability assessments and failure characterization.

Vertical scaling factors were applied to the surface profile to simulate different scaling conditions. Factors below 1 (e.g., 0.1, 0.5) represented suppressed vertical features, while factors above 1 (e.g., 5, 10) represented exaggerated features. The surface profile was adjusted for each scaling factor by multiplying intensity values accordingly. This approach allowed for a systematic evaluation of how vertical scaling affects fractal dimension estimates. The seven fractal analysis methods, implemented in MATLAB, were applied to the scaled images, each providing a unique perspective on surface roughness and scaling effects.

3.1. The Box Counting Method

This method follows Theiler's protocol [9], adapted for image analysis. The failure surface image is converted to grayscale, and grids of various sizes, typically powers of 2 ($2^n \times 2^n$ pixels, where n is an integer), are applied. The number of boxes (n_s) containing surface features is counted for each grid size. A log-log plot $\log_2(n_s)$ against $\log_2(1/r)$ the normalized box size (r) is constructed, and the fractal dimension (D_{BCM}) is calculated from the slope of the plot as:

$$D_{BCM} = \lim_{r \to 0} \frac{\log_2(n_s)}{\log_2(1/r)} \tag{6}$$

3.2. The Differential Box Counting Method

As proposed by Sarkar and Chaudhuri [16], is adapted for our image analysis. For each grid size (s) is calculated:

$$n_i = \left\lceil \frac{M_i - m_i}{I_{\max}/2^m} \right\rceil \tag{7}$$

where M_i and m_i are the maximum and minimum pixel intensities in the i^{th} grid cell, $I_{\max}$ is the image's intensity range, and m is the total number of grid levels. The n_i values are summed across all grid cells for each scale. A log-log plot is then constructed, plotting $\log\left(\sum_i n_i\right)$ versus $\log_2(1/s)$. The fractal dimension (D_{BCM}) is estimated from the slope of this plot.

$$D_{BCM} = \lim_{S\to 0} \frac{\log_2\left(\sum_i n_i\right)}{\log_2(1/s)} \tag{8}$$

3.3. Detrended Fluctuation Analysis

Based on Gu and Zhou [32], is applied through a multi-step process. First, a cumulative sum image is generated by integrating pixel intensities. The image is then partitioned into non-overlapping $s \times s$ squares. A quadratic surface of the form $p(x,y) = a_{00} + a_{10}x + a_{01}y + a_{20}x^2 + a_{11}xy + a_{02}y^2$ is fitted for each square, and the root mean square fluctuation $F(s)$ around this surface is calculated. The average $F(s)$ is computed across all squares of size s, and this process is repeated for various s values. A log-log plot of $\log(F(s))$ versus $\log(s)$ is constructed. The Hurst exponent (H) is determined from the slope of this plot, and the fractal dimension is calculated as:

$$D = 3 - H \tag{9}$$

Integrating multiple fractal analysis methods provides a more nuanced understanding of surface complexity and may reveal method-specific sensitivities to vertical scaling effects.

3.4. Structure-Function Method

The method is employed following the work of Klinkenberg [2]. In this method, the surface roughness profile $Z(x)$ of the failure surface, extracted from the processed JPEG image, is treated as a time series. The structure-function $S(s)$ is computed by evaluating the squared differences in surface heights over a spatial separation s, and it is expected to follow a power-law relationship $S(s) \sim s^W$ where W the power index is. Linear regression of $\log(S(s))$ versus $\log(s)$ provides the value of W, which is then used to estimate the fractal dimension $D = \frac{4-W}{2}$. Vertical scaling factors (λ) are applied to the surface profile to simulate variations in vertical exaggeration or compression, and their effect on the fractal dimension is examined by comparing the estimated D values for different scaling factors.

3.5. The Power Spectrum Method

Based on the theory discussed in [19], this method treats the surface profile $z(x)$

as discrete values. Fourier coefficients $F(u)$ are computed using the Fast Fourier Transform (FFT), and the power spectrum $S(f)$ is calculated for spatial frequencies $S(f) \sim f^{-\alpha}$, where ∝ the scaling exponent is related to surface roughness. Vertical scaling (λ) modifies intensity values, affecting Fourier coefficients and the power spectrum. The fractal dimension (D_f) is estimated from ∝ using:

$$D_f = \frac{d}{2} - \frac{\alpha}{2} \tag{10}$$

3.6. The Variogram Method

Based on Boyd [21], analyzes surface roughness by calculating the variogram $\gamma(h)$ as:

$$\gamma(h) = \frac{1}{2N(h)} \sum_{i=1}^{N(h)} \left[z(x_i) - z(x_i + h) \right]^2 \tag{11}$$

where $N(h)$ the number of data pairs is separated by lag h. The fractal dimension (D_v) is derived from the slope (θ) $\log(\gamma(h))$ versus $\log(h)$ using $D_v = 2 - \theta$ vertical scaling (λ), which alters intensity values and influences the variogram and fractal dimension estimates. Multiple realizations can be used to account for uncertainties.

4. Results and Discussion

4.1. Results

This section presents the results of fractal dimension (FD) estimation methods applied to a slope failure image from the Mashamba opencast mine (see Figure 2). It highlights the influence of vertical scaling on the methods' accuracy, precision, and sensitivity and provides a comparative analysis of their performance.

Figure 2. Slope failure image in Mashamba West Mine.

4.1.1. Grayscale Images and Edge Detection Analysis

Figure 3 presents grayscale images and their corresponding edge-detected outputs under different scaling factors. These visualizations demonstrate how surface complexity changes with scaling, where higher scaling factors amplify vertical features while lower factors suppress them. This qualitative assessment provides a basis for interpreting the sensitivity of different FD estimation methods.

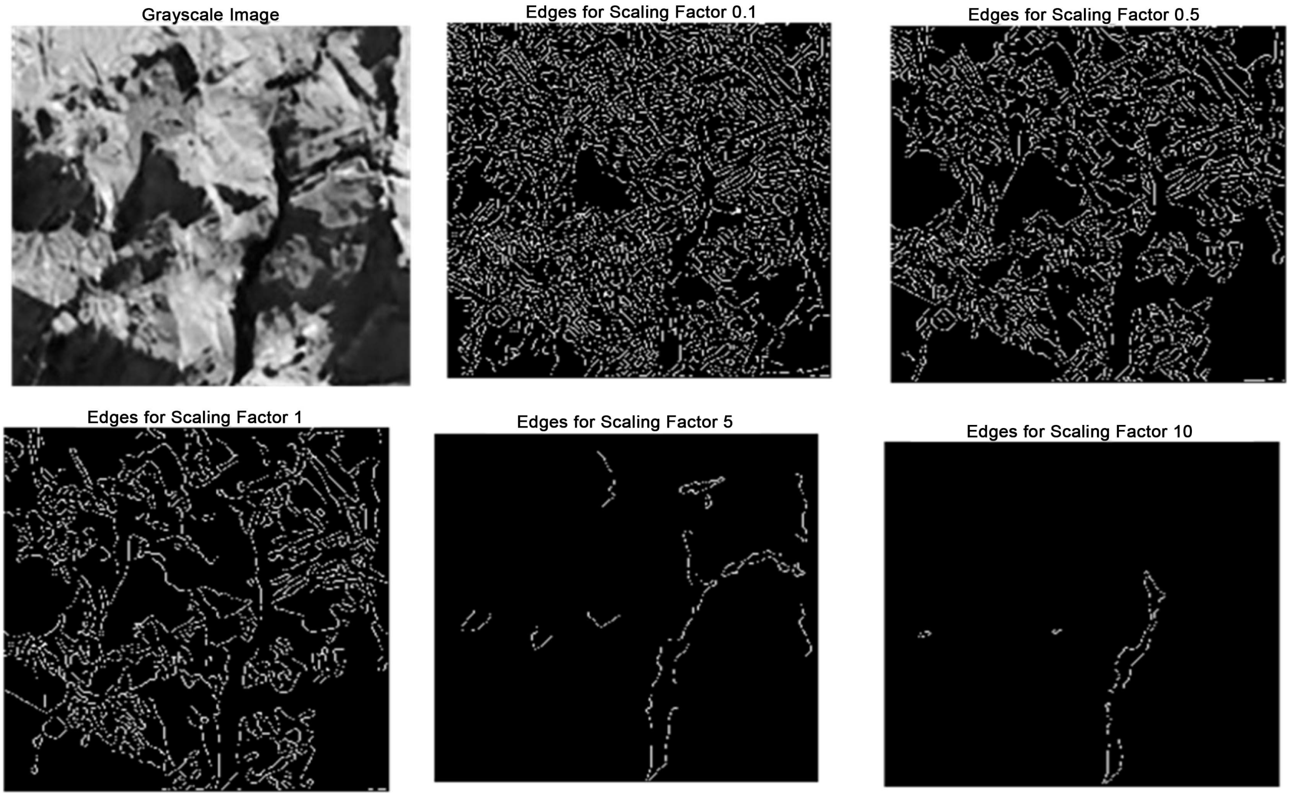

Figure 3. Grayscale images and edge detection outputs for different scaling factors.

4.1.2. Statistical Comparison of Methods

Table 1 summarizes the statistical metrics for each method, including average FD, standard deviation, and range. Variogram and structure-function methods exhibit the highest average FD values (2.7596 and 2.6239, respectively) with minimal variability, making them the most stable methods. TPM produces near-constant FD values (average 2.02494), reflecting its insensitivity to scaling. PS shows a slightly higher average FD (1.4613) with moderate variability, while BCM demonstrates a moderate average FD (1.3537) but with higher variability and range, indicating its sensitivity to scaling. DBC and DFA present moderate average FD values (1.42894 and 1.91576, respectively), with DFA showing more significant variability. These findings highlight PS, Variogram, and Structure Function as stable methods for surface roughness detection. At the same time, BCM and DFA are more volatile, and TPM is ideal for moderately complex surfaces due to its stability.

Figure 4 provides a comparative visualization of each method's average FD, standard deviation, and range. Variogram and structure function (SF) exhibit the highest average FD values with minimal standard deviation and range, confirming their stability and consistency across scaling factors. TPM, however, displays a constant average FD with nearly zero standard deviation and range, indicating its complete independence from scaling. This characteristic of TPM provides a strong reassurance of its stability. BCM and DFA exhibit moderate average FD

Table 1. Statistical summary of FD values for each method.

Method	Average FD	Standard Deviation	Range
BCM	1.3537	0.2886	0.6123
PS	1.4613	0.2675	0.5778
V	2.7596	0.0778	0.1657
SF	2.6239	0.078	0.1787
TPM	2.02494	0.0001943	0.0005
DBC	1.42894	0.4882	1.0737
DFA	1.91576	0.4138	0.9564

values with significant variability, as seen from their larger standard deviations and ranges. PS and DBC demonstrate intermediate behavior, with slightly higher average FD values than BCM and DFA but with less variability. These observations suggest that Variogram and SF are the most stable methods for fractal analysis, while BCM and DFA are more sensitive to scaling changes.

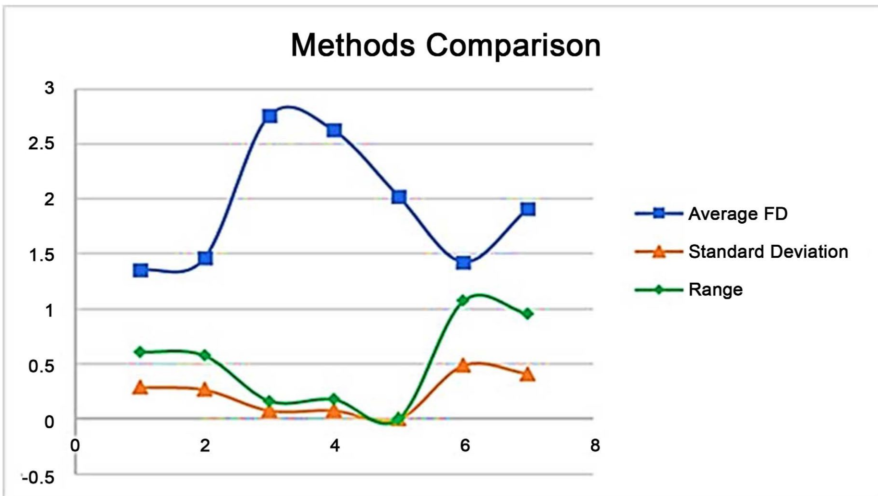

Figure 4. Line graph comparing each method's Average FD, Standard Deviation, and Range.

4.1.3. Fractal Dimension at a Scaling Factor of 0.1

The FD values for all methods at a scaling factor of 0.1 are shown in Figure 5. The Variogram and SF exhibit the highest FD values (2.7044 and 2.5746, respectively), indicating their ability to capture fine-scale surface details and complexity. Conversely, PS provides the lowest FD value (1.2744), reflecting a more conservative surface roughness characterization. BCM, TPM, DBC, and DFA fall between these extremes, with FD values of 1.649, 2.0247, 1.764, and 1.666, respectively. This variation highlights the different sensitivities of methods to scaling and surface properties at fine scales.

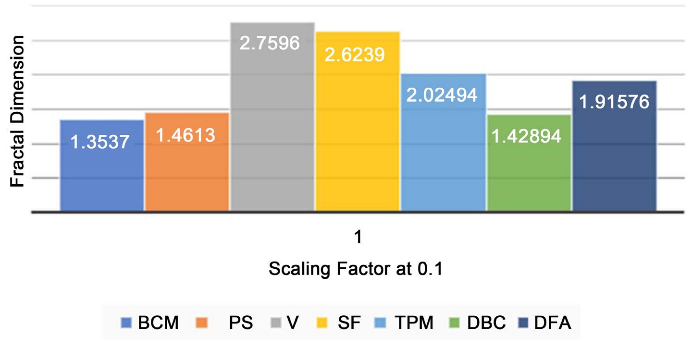

Figure 5. Bar chart of FD values for different methods at scaling factor 0.1.

4.1.4. Dependence of Fractal Dimension on Scaling Factor

The fractal dimension (FD) varies with the scaling factor, revealing distinct patterns that highlight changes in surface complexity. As scaling increases, finer details may diminish, whereas broader structural features become more prominent, influencing FD estimates. These variations underscore the impact of scaling adjustments on the surface roughness characterization. Understanding these dependencies is essential for accurate geotechnical assessments and informed decision making in slope stability analysis.

The Box Counting Method (BCM) estimates the fractal dimension (FD) by analyzing surface roughness through grid-based subdivisions. As the vertical scaling increases, fine-scale features become less distinguishable within larger grid cells, reducing the number of occupied boxes and leading to lower FD values. This decline, as observed in **Figure 6**, from 1.649 at a scaling factor of 0.1 to 1.0367 at 10, reflects BCM's tendency to understate surface complexity at coarser scales due to its sensitivity to resolution-dependent artifacts.

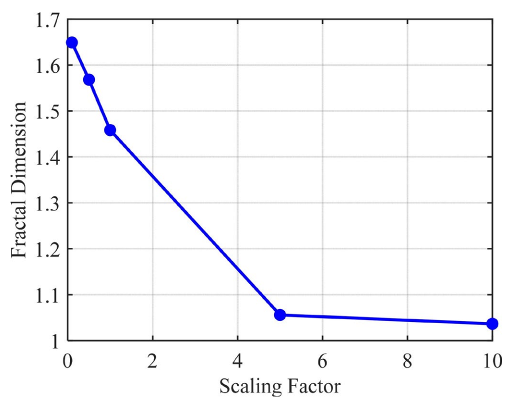

Figure 6. FD vs. scaling factor plot for BCM.

The Power Spectrum (PS) method exhibits a steady increase in fractal dimension (FD) with vertical scaling as the surface roughness shifts from fine-scale irregularities to broader features. This transition alters the frequency distribution, emphasizing lower frequencies and increasing FD values. As shown in **Figure 7**, PS reaches an FD of 1.8522 at a scaling factor of 10, demonstrating its effectiveness in capturing enhanced roughness at larger observational scales.

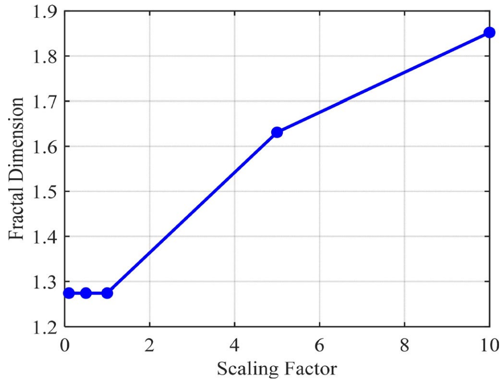

Figure 7. FD vs. scaling factor plot for PS.

The increasing trend of fractal dimension (FD) in the variogram method, as depicted in **Figure 8**, can be attributed to its sensitivity to spatial autocorrelation at varying scales. The variogram quantifies the surface roughness by evaluating the height differences with increasing lag distances, capturing how adjacent points relate to each other. At smaller scaling factors, fine-scale variations dominate, resulting in lower FD values. As the vertical scaling increases, broader surface features become more prominent, extending the correlation structures across larger distances. This transition enhances the ability of the method to detect long-range dependencies, thereby leading to higher FD estimates. The increase from 2.7044 to 2.8701 illustrates its robustness in characterizing surface complexity, making it a reliable tool for analyzing slope failures at coarser resolutions.

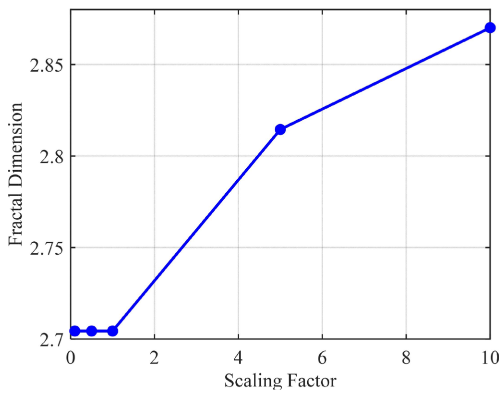

Figure 8. FD vs. scaling factor plot for variogram.

The Structure Function (SF) method detects the surface roughness by analyzing the height variations over different spatial separations. As vertical scaling increases, larger structural features dominate, enhancing long-range correlations in the surface complexity. This results in a gradual increase in FD from 2.5746 to 2.7533, as shown in **Figure 9**, demonstrating SF's sensitivity of SF to scaling effects and its reliability in capturing multi-scale surface characteristics.

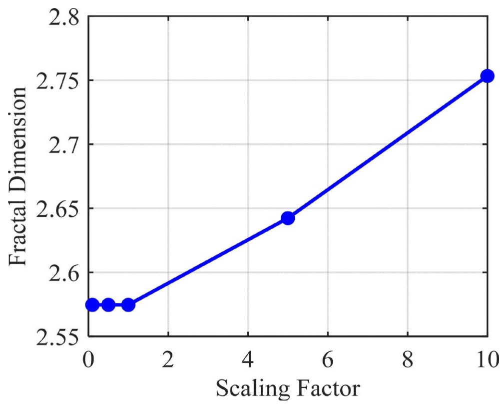

Figure 9. FD vs. scaling factor plot for SF.

The Triangular Prism Method (TPM) maintains nearly constant fractal dimension (FD) values across all scaling factors owing to its inherent geometric approach to estimating surface roughness. Unlike frequency-based methods, TPM calculates the surface area by approximating the terrain with triangular facets, thereby mitigating scaling-induced distortions. This stability suggests that TPM is less affected by vertical exaggeration, providing consistent FD values regardless of scaling adjustments. The moderate sensitivity observed indicates that while TPM captures essential surface characteristics, it does not strongly emphasize vertical irregularities, making it well suited for moderate-complexity surface analyses. As shown in **Figure 10**, its robustness ensures reliable roughness characterization in geotechnical applications.

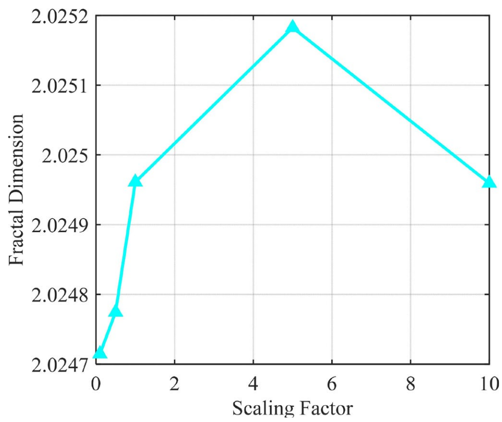

Figure 10. FD vs. scaling factor plot for TPM.

To enhance the reliability of the TPM, empirical validation was conducted across a slope failure surface from a collapse landslide on a steep slope on weathered granite behind the Dinglong Village Committee House, Ganzhou City [37], as shown in **Figure 11**.

Figure 12 presents the fractal dimension (FD) variations obtained using the Triangular Prism Method (TPM) for a collapse landslide on a steep slope in weathered granite behind the Dinglong Village Committee House in Ganzhou

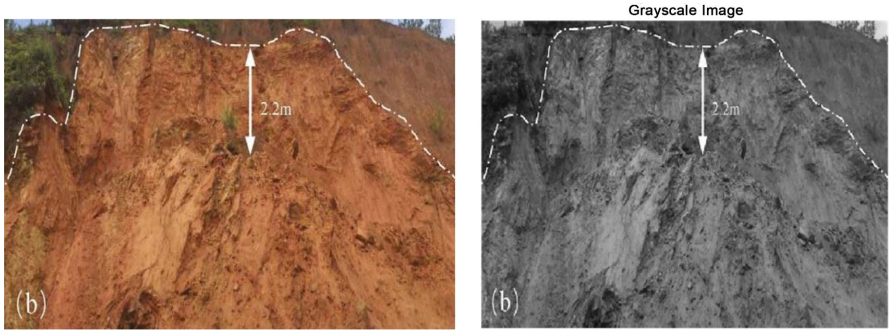

Figure 11. Collapse landslide on a steep slope on weathered granite, behind the Dinglong Village Committee House, Ganzhou City [37].

City. The application of the TPM to this additional failure surface serves as an empirical validation of its ability to maintain scaling independence across different geological conditions. The consistent FD values across scaling factors reinforce TPM's robustness of the TPM in characterizing surface roughness, demonstrating minimal sensitivity to vertical scaling distortions. This stability confirms its suitability for assessing moderate-complexity failure surfaces, ensuring reliable fractal estimates, irrespective of scaling adjustments. The validation further strengthens TPM's applicability of the TPM in geotechnical investigations, affirming its reliability in diverse slope failure scenarios.

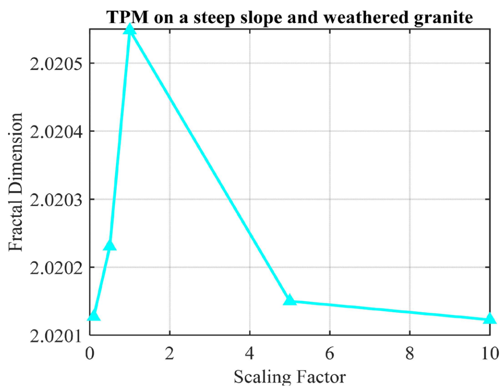

Figure 12. FD vs. scaling factor plot for TPM. Collapse landslide on a steep slope and weathered granite behind the Dinglong Village Committee House, Ganzhou City.

The Differential Box Counting (DBC) method exhibits a sharp decline in the fractal dimension (FD) with increasing vertical scaling owing to its reliance on pixel intensity variations within grid cells. As the scaling factor increases, the vertical exaggeration alters the intensity distribution, reducing the differentiation between adjacent grid levels. This leads to diminished detection of surface complexity, causing the FD to drop significantly, as shown in **Figure 13**. The strong dependence on localized intensity contrasts makes the DBC highly sensitive to scaling effects, limiting its reliability for analyzing rough surfaces at coarser resolutions.

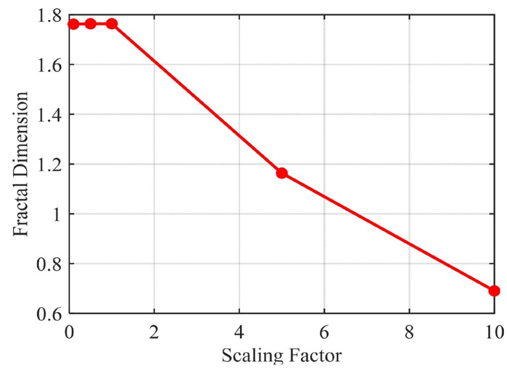

Figure 13. FD vs. scaling factor plot for DBC.

The Detrended Fluctuation Analysis (DFA) method detects long-range correlations in the surface roughness by analyzing fluctuations across different scales. As vertical scaling increases, broader structural variations become more pronounced, enhancing the trend detection in surface complexity. This results in a gradual increase in FD, from 1.666 at a scaling factor of 0.1 to 2.6224 at 10, as shown in Figure 14, demonstrating DFA's sensitivity of the DFA to scaling effects and its ability to capture evolving roughness patterns at coarser resolutions.

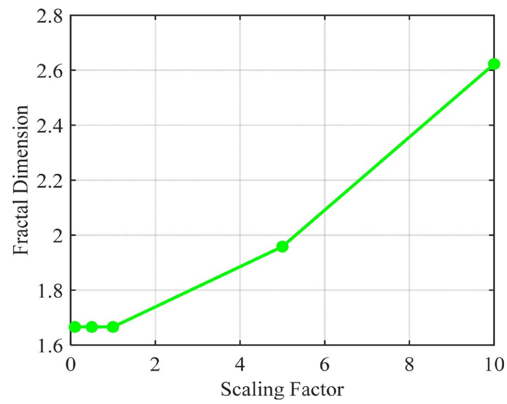

Figure 14. FD vs. scaling factor plot for DFA.

Figure 15 overlays FD trends across all methods and scaling factors, illustrating the methods' divergent responses to scaling changes. BCM and DBC display consistent declines in FD as the scaling factor increases, highlighting their sensitivity to vertical scaling and tendency to understate surface complexity at coarser scales. On the other hand, PS, Variogram, and structure-function (SF) exhibit steep increases in FD with higher scaling factors, reflecting their capability to capture greater surface complexity as the observation scale widens. These methods demonstrate robustness in detecting surface features at larger scales.

Meanwhile, TPM remains nearly constant across all scaling factors, with an FD of approximately 2.025. This stability suggests that TPM is unaffected by scaling and provides reliable surface roughness estimates regardless of the observation scale. Similarly, DFA shows a gradual increase in FD from 1.666 at a scaling factor of 0.1 to 2.6224 at 10, indicating moderate sensitivity to scaling and a tendency to detect increasing complexity at coarser scales.

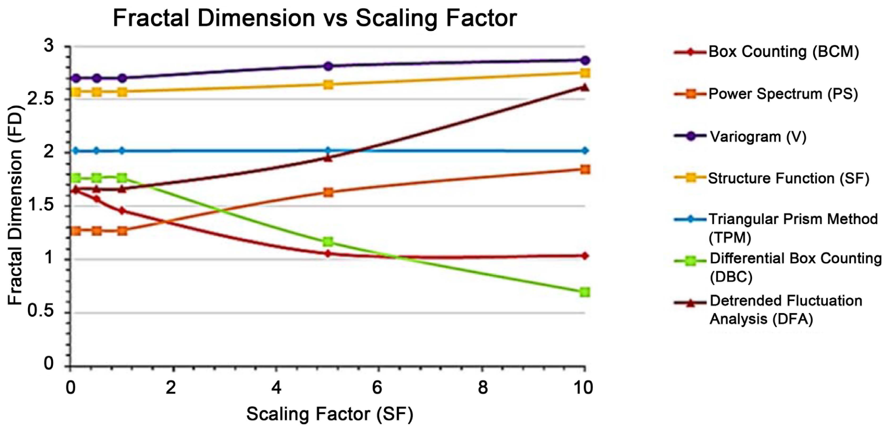

Figure 15. A combined chart shows FD trends across all methods and scaling factors.

4.1.5. Summary and Implications

Table 2 compares all methods' FD values at five scaling factors (0.1, 0.5, 1, 5, 10). PS and variogram consistently produce the highest FD values, capturing greater surface complexity at coarser scales, while BCM and DBC show declining FD, indicating sensitivity to diminishing complexity.

Table 2. FD values for all methods across scaling factors (0.1 - 10).

Scaling Factor	BCM	PS	V	SF	TPM	DBC	DFA
0.1	1.649	1.2744	2.7044	2.5746	2.0247	1.764	1.666
0.5	1.5683	1.2744	2.7044	2.5746	2.0248	1.7635	1.666
1	1.4584	1.2744	2.7044	2.5746	2.025	1.7635	1.666
5	1.056	1.6311	2.8145	2.6423	2.0252	1.1634	1.9584
10	1.0367	1.8522	2.8701	2.7533	2.025	0.6903	2.6224

These results demonstrate that all methods are sensitive to scaling but to varying degrees. PS and variogram are ideal for capturing complex surface characteristics at larger scales, while BCM and DBC are better suited for finer-scale analyses. TPM remains relatively stable across all scales, making it suitable for moderate complexity. These findings emphasize the importance of selecting appropriate methods based on surface characteristics and the desired level of detail in the analysis.

4.2. Discussion

This study evaluated the impact of vertical scaling on fractal dimension (FD) estimation for failure surfaces in opencast mining using seven widely used methods: box-counting method (BCM), power spectrum (PS), Variogram (V), structure function (SF), triangular prism method (TPM), differential box-counting (DBC), and detrended fluctuation analysis (DFA). The findings highlight method-specific sensitivities to vertical scaling, providing insights into their strengths, limitations, and suitability for geotechnical applications. The results align with and, in some cases, diverge from previous research, including the work of Schouwenaars *et al.* [35], offering additional perspectives on FD estimation challenges and solutions.

4.2.1. Vertical Scaling and FD Estimation

The results showed that vertical scaling significantly influences FD estimation, with each method responding differently. BCM and DBC consistently declined FD values as the scaling factor increased. For instance, BCM's FD decreased from 1.649 at a scaling factor of 0.1 to 1.0367 at 10, while DBC's FD dropped from 1.764 to 0.6903 over the same range. This behavior confirms that these methods emphasize fine-scale surface details but become less reliable at coarser scales. Still, PS, Variogram, and SF showed increasing FD values with scaling. PS's FD rose from 1.2744 at 0.1 to 1.8522 at 10, while the Variogram increased from 2.7044 to 2.8701, reflecting their robustness in capturing coarse-scale complexity.

TPM demonstrated nearly constant FD values (2.02) across all scaling factors, suggesting surprising stability. This finding differs from Schouwenaars *et al.* [35], who concluded that TPM is highly sensitive to vertical scaling and achieves scaling independence only under tiny step sizes. The discrepancy may arise from differences in dataset resolution, preprocessing techniques, or scaling ranges. In this study, TPM's stability indicates its potential for reliable application in moderate-complexity surface analyses, where consistency is critical. DFA exhibited a gradual FD increase from 1.666 at 0.1 to 2.6224 at 10, confirming its moderate sensitivity to scaling while balancing fine- and coarse-scale characteristics. The observed differences in method performance are consistent with previous findings, which attribute discrepancies in FD estimates to the mathematical foundations of each method and their numerical implementation. Low-resolution datasets often exacerbate systematic and random errors as methods struggle to preserve the finer details necessary for accurate characterization. These findings highlight the need to consider resolution and scaling simultaneously to achieve reliable FD estimates.

4.2.2. Stability and Method-Specific Sensitivities

The statistical analysis revealed significant differences in the stability of FD estimates across methods. Variogram and SF produced the most consistent results, with minimal variability and high average FD values across scaling factors. For example, the Variogram's standard deviation remained under 0.1 at all scales, indicating its reliability for consistent roughness characterization. PS also demonstrated stability but produced lower FD values at finer scales, indicating a conservative surface roughness characterization. Yet, BCM and DFA exhibited higher variability, with broader standard deviations and ranges. BCM's FD estimates spanned from 1.649 to 1.0367, while DFA, although less variable, still showed wider deviations compared to Variogram or SF. DBC demonstrated moderate variability, performing better at finer scales but remaining sensitive to vertical scaling. The near-constant FD values of TPM across scaling factors underscore its robustness and suitability for moderate complexity analyses, particularly in applications requiring scaling-independent estimates.

4.2.3. Implications of Slope Failure Characterization in Opencast Mines

Given the observed stability of the Variogram and Structure Function (SF) methods across different scales, these techniques should be prioritized for large-scale roughness characterization in opencast mines. Their ability to maintain consistent fractal dimension (FD) values makes them well-suited for identifying large-scale failure zones. In contrast, the Box Counting Method (BCM) and Differential Box Counting (DBC) are more effective for fine-scale analyses, where capturing localized irregularities is critical. The Triangular Prism Method (TPM) exhibits near-constant FD values and provides a reliable approach for moderate complexity assessments, ensuring consistent roughness characterization across varying vertical scaling conditions.

The value of a multi-method approach that integrates PS, Variogram, and SF for large-scale evaluations, while utilizing BCM and DBC for finer-scale assessments, cannot be overstated. This approach significantly enhances the accuracy of failure surface characterization by leveraging the strengths of each method and mitigating their limitations. Future assessment frameworks should also address resolution-dependent biases and incorporate preprocessing techniques such as noise reduction and contrast enhancement. These refinements will improve the reliability of FD estimations and their application in geotechnical analysis.

The findings of this study have practical implications for slope stability analysis in opencast mining. PS, Variogram, and SF demonstrate robustness at larger scales, making them useful for detecting extensive failure zones. Conversely, BCM and DBC excel at identifying fine-scale surface irregularities, which is essential for analyzing localized roughness features. TPM's stability across different scaling factors makes it a reliable option for moderate-complexity characterizations, particularly when a consistent FD estimate is needed regardless of scale. This reiteration of the reliability of the methods instills confidence in the audience about the research findings.

While our study provides valuable insights, it is essential to acknowledge its limitations. The analysis was conducted on a single slope failure at the Mashamba West mine, which, while representative of complex geological conditions, may not fully capture the variability of other mining environments. Therefore, validating these findings across multiple slope failures with diverse geological settings would strengthen their applicability. Additionally, the study focused solely on vertical scaling without examining the combined effects of vertical and horizontal scaling, which are critical for characterizing anisotropic surfaces. Future research should investigate these interactions and their influence on FD estimates. Lastly, while preprocessing techniques were consistently applied, their impact on noise reduction and resolution enhancement was not explored in depth. Addressing these aspects in future studies can further improve the accuracy and applicability of FD estimation methods in geotechnical applications.

5. Conclusion

This study investigated the impact of vertical scaling on fractal dimension (FD) estimation for slope failures in opencast mining, using seven widely recognized methods. The results showed that BCM and DBC exhibit consistent declines in FD estimates with increasing scaling factors, emphasizing their focus on fine-scale details but highlighting their limitations in coarse-scale analyses. Conversely, PS, variogram, and SF demonstrated increasing FD values with scaling, reflecting their robustness in capturing coarse-scale surface complexity. TPM provided nearly constant FD values across all scaling factors, showing unexpected stability and suggesting its suitability for moderate-complexity surface analyses. DFA displayed a gradual increase in FD values, striking a balance between fine- and coarse-scale sensitivity. The findings align with existing literature in identifying the influence of scaling on FD estimation while also uncovering unique behaviors for methods like TPM and DFA. Variogram and SF emerged as the most stable methods, offering reliable FD estimates with minimal variability, whereas BCM and DFA displayed more significant variability across scaling factors. The research underscores the need to select fractal analysis methods based on the scale of interest and the surface characteristics, as no single method is universally optimal for all applications. These insights are critical for accurately characterizing slope failures in practical geotechnical applications. Robust methods like variogram and SF are better suited for large-scale roughness analysis, while BCM and DBC are ideal for fine-scale assessments. TPM's stability across scaling factors makes it a reliable option for moderate-complexity applications requiring consistent estimates. These findings contribute to improved surface roughness characterization in opencast mining by addressing the specific scaling and surface complexity requirements.

Acknowledgments

The authors sincerely thank Sicomines Company for its invaluable contribution to this research.

Conflicts of Interest

The authors declare that they have no conflicts of interest to disclose.

References

[1] Xu, T., Moore, I.D. and Gallant, J.C. (1993) Fractals, Fractal Dimensions and Landscapes—A Review. *Geomorphology*, **8**, 245-262. https://doi.org/10.1016/0169-555x(93)90022-t

[2] Klinkenberg, B. (1994) A Review of Methods Used to Determine the Fractal Dimension of Linear Features. *Mathematical Geology*, **26**, 23-46.

https://doi.org/10.1007/bf02065874

[3] Lopes, R. and Betrouni, N. (2009) Fractal and Multifractal Analysis: A Review. *Medical Image Analysis*, **13**, 634-649. https://doi.org/10.1016/j.media.2009.05.003

[4] Cherepanov, G.P., Balankin, A.S. and Ivanova, V.S. (1995) Fractal Fracture Mechanics—A Review. *Engineering Fracture Mechanics*, **51**, 997-1033. https://doi.org/10.1016/0013-7944(94)00323-a

[5] Majumdar, A. and Bhushan, B. (1990) Role of Fractal Geometry in Roughness Characterization and Contact Mechanics of Surfaces. *Journal of Tribology*, **112**, 205-216. https://doi.org/10.1115/1.2920243

[6] De Chiffre, L., Lonardo, P., Trumpold, H., Lucca, D.A., Goch, G., Brown, C.A., *et al.* (2000) Quantitative Characterisation of Surface Texture. *CIRP Annals*, **49**, 635-652. https://doi.org/10.1016/s0007-8506(07)63458-1

[7] Nayak, S.R., Mishra, J. and Jena, P.M. (2018) Fractal Dimension of Grayscale Images. In: Pattnaik, P.K., *et al.*, Eds., *Progress in Computing*, *Analytics and Networking*, Springer, 225-234. https://doi.org/10.1007/978-981-10-7871-2_22

[8] Nayak, S.R., Mishra, J. and Palai, G. (2019) Analysing Roughness of Surface through Fractal Dimension: A Review. *Image and Vision Computing*, **89**, 21-34. https://doi.org/10.1016/j.imavis.2019.06.015

[9] Theiler, J. (1990) Estimating Fractal Dimension. *Journal of the Optical Society of America A*, **7**, Article No. 1055. https://doi.org/10.1364/josaa.7.001055

[10] Lam, N.S., Qiu, H., Quattrochi, D.A. and Emerson, C.W. (2002) An Evaluation of Fractal Methods for Characterizing Image Complexity. *Cartography and Geographic Information Science*, **29**, 25-35. https://doi.org/10.1559/152304002782064600

[11] Ai, T., Zhang, R., Zhou, H.W. and Pei, J.L. (2014) Box-Counting Methods to Directly Estimate the Fractal Dimension of a Rock Surface. *Applied Surface Science*, **314**, 610-621. https://doi.org/10.1016/j.apsusc.2014.06.152

[12] Foroutan-pour, K., Dutilleul, P. and Smith, D.L. (1999) Advances in the Implementation of the Box-Counting Method of Fractal Dimension Estimation. *Applied Mathematics and Computation*, **105**, 195-210. https://doi.org/10.1016/s0096-3003(98)10096-6

[13] Li, J., Du, Q. and Sun, C. (2009) An Improved Box-Counting Method for Image Fractal Dimension Estimation. *Pattern Recognition*, **42**, 2460-2469. https://doi.org/10.1016/j.patcog.2009.03.001

[14] Panigrahy, C., Seal, A., Mahato, N.K. and Bhattacharjee, D. (2019) Differential Box Counting Methods for Estimating Fractal Dimension of Gray-Scale Images: A Survey. *Chaos*, *Solitons & Fractals*, **126**, 178-202. https://doi.org/10.1016/j.chaos.2019.06.007

[15] Panigrahy, C., Seal, A. and Mahato, N.K. (2020) Image Texture Surface Analysis Using an Improved Differential Box Counting Based Fractal Dimension. *Powder Technology*, **364**, 276-299. https://doi.org/10.1016/j.powtec.2020.01.053

[16] Sarkar, N. and Chaudhuri, B.B. (1994) An Efficient Differential Box-Counting Approach to Compute Fractal Dimension of Image. *IEEE Transactions on Systems*, *Man*, *and Cybernetics*, **24**, 115-120. https://doi.org/10.1109/21.259692

[17] Marx, E., Malik, I.J., Strausser, Y.E., Bristow, T., Poduje, N. and Stover, J.C. (2002) Power Spectral Densities: A Multiple Technique Study of Different Si Wafer Surfaces. *Journal of Vacuum Science & Technology B*: *Microelectronics and Nanometer Structures Processing*, *Measurement*, *and Phenomena*, **20**, 31-41. https://doi.org/10.1116/1.1428267

[18] Wen, R. and Sinding-Larsen, R. (1997) Uncertainty in Fractal Dimension Estimated from Power Spectra and Variograms. *Mathematical Geology*, **29**, 727-753. https://doi.org/10.1007/bf02768900

[19] Solomon Jr, O.M. (1991) PSD Computations Using Welch's Method. Power Spectral Density (PSD), SAND-91-1533.

[20] Chen, Z., Liu, Y. and Zhou, P. (2018) A Comparative Study of Fractal Dimension Calculation Methods for Rough Surface Profiles. *Chaos*, *Solitons & Fractals*, **112**, 24-30. https://doi.org/10.1016/j.chaos.2018.04.027

[21] Boyd, D.L., Trainor-Guitton, W. and Walton, G. (2018) Assessment of Rock Unit Variability through Use of Spatial Variograms. *Engineering Geology*, **233**, 200-212. https://doi.org/10.1016/j.enggeo.2017.12.012

[22] Jiandong, X., Chiente, L. and JACOBI, R.D. (2002) Characterizing Fracture Spatial Patterns by Using Semivariograms. *Acta Geologica Sinica-English Edition*, **76**, 89-99. https://doi.org/10.1111/j.1755-6724.2002.tb00074.x

[23] Oliver, M.A. and Webster, R. (1986) Semi-Variograms for Modelling the Spatial Pattern of Landform and Soil Properties. *Earth Surface Processes and Landforms*, **11**, 491-504. https://doi.org/10.1002/esp.3290110504

[24] De Santis, A., Fedi, M. and Quarta, T. (1997) A Revisitation of the Triangular Prism Surface Area Method for Estimating the Fractal Dimension of Fractal Surfaces. *Annals of Geophysics*, **40**. https://doi.org/10.4401/ag-3882

[25] Clarke, K.C. (1986) Computation of the Fractal Dimension of Topographic Surfaces Using the Triangular Prism Surface Area Method. *Computers & Geosciences*, **12**, 713-722. https://doi.org/10.1016/0098-3004(86)90047-6

[26] Sun, W. (2006) Three New Implementations of the Triangular Prism Method for Computing the Fractal Dimension of Remote Sensing Images. *Photogrammetric Engineering & Remote Sensing*, **72**, 373-382. https://doi.org/10.14358/pers.72.4.373

[27] Zhou, Y., Fung, T. and Leung, Y. (2016) Improved Triangular Prism Methods for Fractal Analysis of Remotely Sensed Images. *Computers & Geosciences*, **90**, 64-77. https://doi.org/10.1016/j.cageo.2016.02.018

[28] Hargittai, I. (2024) Remembering Benoit Mandelbrot on His Centennial—His Fractal Geometry Changed Our View of Nature. *Structural Chemistry*, **35**, 1657-1661. https://doi.org/10.1007/s11224-024-02290-9

[29] Kirkby, M.J. (1983) The Fractal Geometry of Nature. Benoit B. Mandelbrot. W. H. Freeman and Co., San Francisco, 1982. No. of Pages: 460. Price: £22.75 (Hardback). *Earth Surface Processes and Landforms*, **8**, 406-406. https://doi.org/10.1002/esp.3290080415

[30] Mandelbrot, B.B. and Van Ness, J.W. (1968) Fractional Brownian Motions, Fractional Noises and Applications. *SIAM Review*, **10**, 422-437. https://doi.org/10.1137/1010093

[31] Petrosky, T., Kotaka, D. and Tanaka, S. (2022) Mandelbrot's Fractal Structure in Decaying Process of a Matter-Field Interacting System. In: Brenig, L., Brilliantov, N. and Tlidi, M., Eds., *Fundamental Theories of Physics*, Springer International Publishing, 59-70. https://doi.org/10.1007/978-3-031-04458-8_4

[32] Gu, G. and Zhou, W. (2006) Detrended Fluctuation Analysis for Fractals and Multifractals in Higher Dimensions. *Physical Review E*, **74**, Article ID: 061104. https://doi.org/10.1103/physreve.74.061104

[33] Morales Martínez, J.L., Segovia-Domínguez, I., Rodríguez, I.Q., Horta-Rangel, F.A. and Sosa-Gómez, G. (2021) A Modified Multifractal Detrended Fluctuation Analysis

(MFDFA) Approach for Multifractal Analysis of Precipitation. *Physica A*: *Statistical Mechanics and Its Applications*, **565**, Article ID: 125611. https://doi.org/10.1016/j.physa.2020.125611

[34] Hurst, H.E. (1951) Long-term Storage Capacity of Reservoirs. *Transactions of the American Society of Civil Engineers*, **116**, 770-799. https://doi.org/10.1061/taceat.0006518

[35] Schouwenaars, R., Jacobo, V.H. and Ortiz, A. (2017) The Effect of Vertical Scaling on the Estimation of the Fractal Dimension of Randomly Rough Surfaces. *Applied Surface Science*, **425**, 838-846. https://doi.org/10.1016/j.apsusc.2017.07.083

[36] Alvarez-Ramirez, J., Echeverria, J.C. and Rodriguez, E. (2008) Performance of a High-Dimensional Method for Hurst Exponent Estimation. *Physica A*: *Statistical Mechanics and Its Applications*, **387**, 6452-6462. https://doi.org/10.1016/j.physa.2008.08.014

[37] Zhan, Q., Wang, S., Wang, L., Guo, F., Zhao, D. and Yan, J. (2021) Analysis of Failure Models and Deformation Evolution Process of Geological Hazards in Ganzhou City, China. *Frontiers in Earth Science*, **9**, Article ID: 731447. https://doi.org/10.3389/feart.2021.731447